Pattern-motion responses in human visual cortex

Alexander C. Huk[1,2] and David J. Heeger[1]

[1] *Psychology Department, Stanford University, Stanford, California 94305-2130, USA*

[2] *Current address: Department of Physiology and Biophysics, University of Washington, Box 357290, Health Sciences Bldg, Room G-424, Seattle, Washington 98195-7290, USA*

Correspondence should be addressed to A.H. (huk@u.washington.edu)

Published online: 3 December 2001, DOI: 10.1038/nn774

Physiological models of visual motion processing posit that 'pattern-motion cells' represent the direction of moving objects independent of their particular spatial pattern. We performed fMRI experiments to identify neuronal activity in the human brain selective for pattern motion. A protocol using adaptation to moving 'plaid' stimuli allowed us to separate pattern-motion responses from other types of motion-related activity within the same brain structures, and revealed strong pattern-motion selectivity in human visual area MT+. Reducing the perceptual coherence of the plaids yielded a corresponding decrease in pattern-motion responsivity, providing evidence that percepts of coherent motion are closely linked to the activity of pattern-motion cells in human MT+.

A key stage in the perception of visual motion is the representation of the speed and direction of moving objects independent of their particular spatial pattern. Single-neuron electrophysiology experiments in the visual cortex of macaque monkeys and cats have identified 'component-motion cells,' which respond to the direction of motion orthogonal to local contours, and 'pattern-motion cells,' which respond to the direction of motion independent of the orientations of contours making up the stimulus pattern[1–4]. In primary visual cortex (V1), all the motion-selective neurons are component-motion cells, whereas populations of pattern-motion cells have been identified in extrastriate visual areas including the middle temporal region (known as MT or V5). To date, there is no clear physiological evidence for pattern-motion cells in the human brain. Furthermore, although pattern-motion cell physiology is consistent with pattern-motion perception, the link between the two has been inferred from human judgments of the subjective perceptual appearance of motion on the one hand and monkey electrophysiology on the other[5]. Here we describe functional magnetic resonance imaging (fMRI) experiments demonstrating that human visual area MT+ exhibits strong responses to pattern motion, and that changes in these pattern-motion responses correspond to changes in human observers' percepts of pattern motion.

Electrophysiological and psychophysical studies have separated component- and pattern-motion responsivity by using 'plaid' stimuli composed of two superimposed moving gratings with different orientations[1,6–10]. These plaid patterns typically appear to drift coherently in a single direction that can be predicted from the motions of the component gratings by a simple calculation (the 'intersection of constraints'). However, when the spatial frequencies of the two gratings are sufficiently different, plaids lose perceptual coherence, that is, they are perceived as two transparent gratings sliding over one another[6,11].

In our fMRI experiments, we used adaptation to plaid stimuli to separate pattern-motion responses from component-motion responses. To examine the relationship between pattern-motion responsivity and the percept of coherent pattern motion, we adjusted the relative spatial frequencies of our component gratings to reduce perceptual coherence and tested for a corresponding change in pattern-motion adaptation.

Results

We measured fMRI signals (GE 3T scanner, custom surface coil, 12 axial slices covering the occipital lobe and the posterior temporal and parietal lobes, $3.2 \times 3.2 \times 4$ mm voxel size, 0.67-Hz frame rate) from visual cortex while subjects viewed a sequence of moving plaid stimuli. Each plaid was composed of two superimposed gratings picked from a set of four sinusoidal component gratings. During adapted-direction blocks, gratings were paired to produce plaids that all appeared to move in the same direction (**Fig. 1a**); during mixed-direction blocks, the same component gratings were recombined in different pairings to produce plaids that appeared to move in different directions from trial to trial, excluding the adapted direction (**Fig. 1b**). Critically, each component grating was shown the same number of times in both blocks. Thus, pattern-motion cell responses would be expected to decrease during adapted-direction blocks compared to mixed-direction blocks. Component-motion cells, however, would be expected to show the same degree of adaptation during both blocks. The fMRI response would therefore be expected to modulate (decreasing during adapted-direction blocks, rising during mixed-direction blocks) only in visual areas with large subpopulations of pattern-motion cells. To control attention, subjects performed a speed discrimination judgment on each stimulus presentation (see Methods).

Pattern-motion adaptation produced strong modulations of the fMRI responses in extrastriate visual area MT+ (**Fig. 2a**, solid trace). This area of the human brain is believed to be homologous to macaque MT and adjacent motion-selective areas. To compare across different visual areas, we calculated a

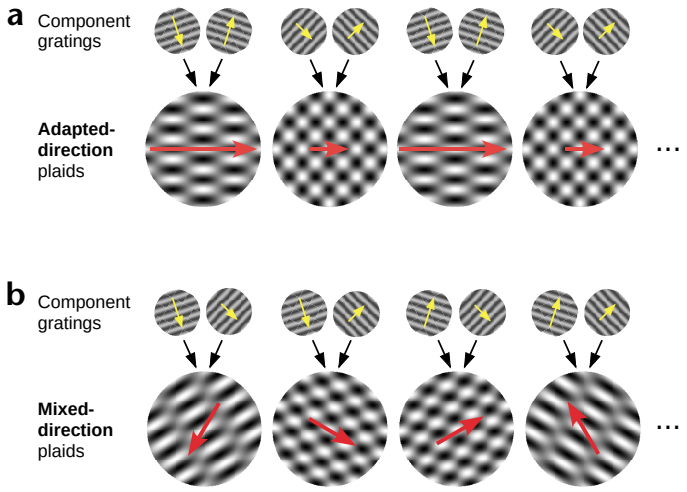

Fig. 1. Stimuli and protocol for coherent-plaid adaptation experiment. (**a**) Adapted-direction block. Component gratings (top) were paired to produce a series of plaid stimuli that all appeared to move in the same direction (bottom). Yellow arrows, component grating motions. Red arrows, perceived direction of plaid pattern motions (as computed by the intersection of constraints). Length of each arrow is approximately proportional to speed. (**b**) Mixed-direction block. The same component gratings were recombined in different pairings (top) to produce a series of plaids with directions that varied from trial to trial (bottom).

pattern-motion adaptation index, dividing the response amplitudes (see Methods) from the pattern-motion adaptation experiment by the response amplitudes measured in a separate baseline experiment (in which the stimulus alternated between moving dots and a blank display). This calculation was performed separately for each subject and each visual area, and then averaged across subjects. The index confirms that pattern-motion adaptation was strongest in MT+ and weakest in V1 (**Fig. 2b**). Other extrastriate visual areas showed intermediate levels of pattern-motion adaptation.

To test for a relationship between these pattern-motion responses and the percept of coherent pattern motion, we adjusted the spatial frequencies of the component gratings so that they differed by three octaves within each plaid. Consistent with previous psychophysical findings, subjects now reported that the two superimposed gratings typically appeared to slide, transparently and independently, across one another. We reasoned that if the activity of pattern-motion cells is tightly linked to the percept of coherent plaid motion, then pattern-motion cells should show a weaker response and a correspondingly weaker adaptation effect during perceptual transparency.

Transparent component motion yielded a substantial reduction of adaptation (**Fig. 2a**, dashed trace). This reduction was statistically significant in all extrastriate visual areas (MT+, $F_{1,67} = 18.52$, $p < 0.0001$; V3A, $F_{1,67} = 16.99$, $p < 0.0001$; V4v, $F_{1,67} = 6.09$; $p < 0.05$; V3, $F_{1,67} = 13.08$, $p < 0.0005$; V2, $F_{1,67} = 16.21$, $p < 0.0005$; repeated-measures ANOVA on the fMRI response amplitudes from the pattern-motion and transparent component-motion experiments, calculated separately for each visual area). The motion adaptation index confirms that adaptation in MT+ was much smaller for transparent component motion than for coherent pattern motion (**Fig. 2b**, compare white and gray bars), demonstrating that the pattern-motion selective activity in MT+ is indeed linked to the percept of coherent plaid motion. This was not the case for V1, where responses were small and approximately equal in the pattern- and component-motion experiments ($F_{1,67} = 0.75$, $p = 0.39$).

A control experiment confirmed that the large reduction in MT+ adaptation did not result simply from a weak response to the higher and lower spatial frequencies used in the transparent, component-motion experiment. We repeated the measurements with high and low spatial frequency gratings, but instead of mixing the spatial frequencies of the two gratings on each trial (which produced the transparent component stimuli), we matched the spatial frequencies (to produce coherent plaid stimuli). Using these high-frequency plaids and low-frequency plaids yielded adaptation effects in MT+ very similar to those in the original pattern-motion adaptation experiment ($F_{1,55} = 0.07$, $p = 0.93$).

The small response observed in all visual areas in the transparent component-motion experiment (**Fig. 2b**, all white bars are roughly the same height) may reflect a nonspecific effect of presenting repeated stimuli compared to varied ones. Regardless, the critical factor is that area MT+ showed much stronger adaptation to coherent pattern motion than to transparent component motion, demonstrating that changes in its responses reflect changes in the perception of pattern motion. Although we also observed a small effect in V1 when viewing either coherent pattern motion or transparent component motion, the lack of a difference between these two conditions suggests that V1 neurons are not critically linked to the perception of coherent pattern motion.

We also performed a control experiment to rule out the possibility that our results might be explained by motion-opponent mechanisms, mutually suppressive populations of neurons sensitive to motions in opposite directions[12]. In our main experiment, the adapted-direction block consisted of plaids with separations of 144° and 90°; the mixed-direction block consisted of plaids with separations of 27° and 117°. If the plaid of 144° engaged opponent mechanisms, responses to the adapted-direction block would be smaller, independent of any direction-selective pattern-motion adaptation. We therefore performed a series of measurements in which we alternated between blocks of wide-angle plaids (the widest, 144° plaid from the original experiment) and narrow-angle plaids (the narrowest, 27° plaid from the original experiment). (Note that the remaining plaids had components that were approximately perpendicular and were wider in the mixed-direction blocks.) On each trial, the plaid direction was rotated by multiples of 90°, to minimize adaptation, yielding only a comparison between the stimulus most expected to engage opponency (widest plaid) and the stimulus least expected to engage opponency (narrowest plaid). We found that MT+ response modulations were not statistically different from zero (subject A.C.H., $p = 0.28$; A.R.W., $p = 0.19$, trend in direction opposite that predicted by motion opponency; D.J.H., $p = 0.75$; two-tailed t-test), demonstrating that opponency is not a confound for the interpretation of our main experiment. We note that a similar number of repetitions produced highly significant modulations of MT+ activity in the main pattern-motion adaptation experiment.

We performed a further control experiment to rule out any other possible confounds related to non-directional differences between the plaids in the two blocks of the main experiment. (For example, the plaid patterns in one block moved faster on average than those in the other block.) We presented all the plaids from the original experiment, but rotated their directions by mul-

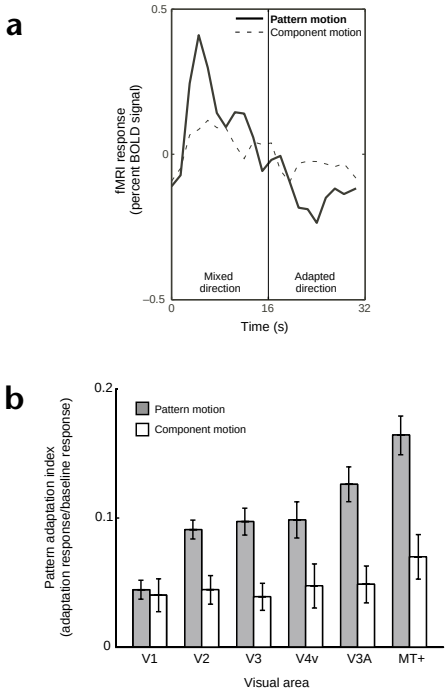

Fig. 2. Pattern-motion adaptation in human visual cortex. (**a**) Average time series in MT+. Pattern-motion adaptation produced strong modulations in MT+ activity. Transparent component motion evoked much less adaptation. Each trace represents the average MT+ response, averaged across subjects and scanning sessions. (**b**) Adaptation index across all visual areas. Pattern-motion adaptation was largest in MT+, but also evident in other extrastriate visual areas. Adaptation was weak and roughly equal across visual areas in the transparent component-motion experiment. Height of bars, geometric mean across subjects (arithmetic mean yielded similar results). Error bars, bootstrap estimates of the 68% confidence intervals.

tiples of 90° from trial to trial to minimize adaptation. The response modulations in MT+ were not significantly different from zero (A.C.H., $p = 0.35$; D.J.H., $p = 0.74$, two-tailed t-test), demonstrating that the two blocks of plaids elicited similar response levels when the effects of both component- and pattern-motion adaptation were absent. This result provides further evidence that adaptation, due to the repetition of pattern direction, was the key factor in the original experiment.

Discussion

Our findings demonstrate that human MT+ contains a population of pattern-motion cells and that the activity of those neurons is linked to the perception of coherent pattern motion. The pattern-motion responsivity of human MT+ adds to the case for a homology to macaque MT, which includes a relatively large proportion of pattern-motion cells[1]. We also observed lesser degrees of pattern-motion adaptation in V2, V3, V3A and V4v. Macaque V3 is known to have a minority of pattern-motion cells[13], but there are no published investigations of pattern-motion cells in macaque V2, V3A or V4. Although our data demonstrate pattern-motion responses in each of these visual areas, we cannot determine if pattern motion is computed separately in each visual area or if the responses in V2–V4 are affected by the adaptation that is taking place in MT+. We emphasize that fMRI adaptation studies[14–17] can reveal the selectivities of subpopulations of neurons in the human brain, even when those neurons are intermingled at a spatial scale that is finer than the spatial sampling resolution (voxel size) of the fMRI measurements.

Methods

We collected fMRI data in 3 subjects, males, 25–39 years old, all with normal or corrected-to-normal vision. Experiments were undertaken with the written consent of each subject, and in compliance with the safety guidelines for MR research. Each subject participated in several scanning sessions: one to obtain a high-resolution anatomical volume, one to identify MT+, one to identify the retinotopically organized cortical visual areas, 2–3 to measure motion adaptation, one to measure baseline responses and 1–3 to perform control measurements. In each subject, we collected 8–20 repeats of the pattern-motion adaptation experiment and 8–16 repeats of the various control experiments.

Stimulus and protocol. Stimuli were presented on a flat-panel display (NEC, multisynch LCD 2000, Itasca, Illinois) placed within a Faraday box with a conducting glass front, positioned near the subjects' feet. Subjects lay on their backs in the MR scanner and viewed the display through binoculars.

Subjects viewed a pair of circular patches 12° in diameter centered 7.5° to the left and right of a central fixation point. Patches were filled with a plaid stimulus comprised of two superimposed sinusoidal gratings. Individual component gratings had 20% contrast, and spatial and temporal frequencies were selected to yield a variety of pattern directions when superimposed in various combinations (**Fig. 1**).

Each scan consisted of 6 (32-s) cycles; each cycle consisted of alternating adapted-direction and mixed-direction blocks. Adapted-direction blocks consisted of 8 consecutive trials in which the plaid stimulus always appeared to move in the same direction (horizontally, at 12.9 or 1.9°/s; **Fig. 1a**); mixed-direction blocks consisted of 8 trials in which the direction of the plaids varied from trial-to-trial (possible plaid directions, computed from the intersection-of-constraints of the component gratings, were ±31°, ±123° from horizontal at 5.3°/s and 6.3°/s; **Fig. 1b**). The component gratings with orientations of ±72° had spatial frequencies of 0.5 cycles/degree and temporal frequencies of 2 cycles/second (**Fig. 1a**, components above first plaid); the component gratings with orientations ±45° had spatial frequencies of 0.5 cycles/degree and temporal frequencies of 0.67 cycles/second (**Fig. 1a**, components above second plaid). In the component-motion experiment, perceptual transparency was achieved by scaling one component's spatial frequency up to 1 cycle/degree and the other down to 0.125 cycle/degree, producing a 3-octave separation. (Temporal frequencies were also scaled accordingly to leave component velocities unchanged.)

To control attention, subjects performed a speed discrimination judgment on each stimulus presentation[16]. Each 2-s trial consisted of 1300 ms of plaid motion followed by a 700-ms luminance-matched blank period during which subjects pressed a button to indicate which plaid (left or right of fixation) moved faster. The speed differences were determined by an adaptive staircase procedure, adjusting the speeds from trial to trial so that subjects would be approximately 80% correct.

Across different blocks and experiments, we chose to equate percent-correct performance, instead of the exact stimulus speed (although speeds did remain within a few percent), because in previous work, we and others have noted large attentional effects on MT+ responses, but no effects of slight differences in speed[18–20]. Although the speed discrimination thresholds were larger for non-coherent (transparent gratings) than for coherent plaids (but not for mixed- versus adapted-direction blocks), the differences were not very large (percent speed-increment thresholds were ~15% versus ~10% for non-coherent versus coherent, respectively). These small speed differences might affect the responses of some individual neurons (although speed tuning curves of all direction-selective cells are rather broad), but these speed differences would not be expected to evoke measurable changes in the pooled activity (as measured with fMRI) of large populations of neurons.

In the adaptation experiments, equal numbers of scans were collected with the plaids moving in opposite directions (for example, inward

toward fixation and outward away from fixation). Averaging across scans, and hence across adapting direction, ensured that our measurements of adaptation-related responses were not confounded with an inherently stronger response to any particular direction of motion.

fMRI data acquisition. MR imaging was performed using a 3T GE scanner with a custom-designed dual surface coil. A bite bar stabilized the subjects' heads. Subjects viewed the stimuli while a time series of fMRI volumes were acquired (every 1.5 s) using a T2*-sensitive, spiral-trajectory, gradient-echo pulse sequence[21] (TE, 30 ms; TR, 750 ms (2 interleaves); FA, 55°; FOV, 220 mm; effective inplane pixel size, 3.2 × 3.2 mm; 4-mm slice thickness, 12 slices). Slice orientation was either pseudo-axial (adaptation and control experiments) or coronal (baseline measurements). The 12 pseudo-axial or coronal slices covered the retinotopic visual areas and extended rostrally to include MT+.

Each MR scanning session began by acquiring a set of anatomical images using a T1-weighted SPGR pulse sequence in the same slices as the functional images (FOV, 220 mm; TR, 68 ms; TE, 15 ms; echo-train length, 2). The inplane anatomical images were aligned to a high-resolution anatomical volume of each subject's brain so that all MR images (across multiple scanning sessions) from a given subject were coregistered with an accuracy of approximately 1 mm (ref. 22).

Defining the visual areas. The fMRI data were analyzed in each of several visual cortical areas, defined separately in each subject. MT+ was identified as a contiguous region of gray matter in the occipital extension of the inferior temporal sulcus that responded more strongly to full-field moving dots than to a stationary dot pattern[23–25]. Retinotopically organized visual areas (V1, V2, V3, V3A, V4v) were defined by measuring the polar angle component of the cortical retinotopic map[26–29].

The gray matter regions corresponding to MT+ and the retinotopic areas were further delimited based on the responses to a reference scan. The reference scan responses were used to exclude unresponsive voxels such as gray matter regions that would have responded to visual field locations outside the stimulus apertures, or voxels that had too little overlap with gray matter. A reference scan was run during each scanning session. During the reference scan, subjects fixated while the display alternated between 16 s of moving dots and 16 s of stationary dots (presented in the same patches as the adaptation experiments). Voxels that were not strongly correlated with the stimulus alternations ($r < 0.50$, 0–8-s time lag) were discarded from further analysis. Correlation thresholds ranging from 0.20–0.70 yielded similar results.

fMRI data analysis. Data from the first block of each fMRI scan were discarded to allow the adaptation state to stabilize and to allow the hemodynamic response to reach steady state. The fMRI time series were preprocessed by high-pass filtering the time series at each voxel (which attenuated frequencies below 0.00714 Hz by greater than 90%, noting that the block alternation frequency was 1/32 = 0.03125 Hz) to compensate for the slow signal drift typical in fMRI signals[30], and by dividing each voxel's time series by its mean intensity. The resulting time series were averaged throughout the gray matter corresponding to each visual area's representation of the stimulus.

Response amplitudes were calculated using techniques described in detail elsewhere[12,20]. Briefly, the mean time series in each visual area during each scan was fit with a sinusoid with the same period as the block-alternation period (32 s), and we extracted the amplitude component of this best-fitting sinusoid while compensating for the hemodynamic delay. The resulting response amplitudes were positive when the responses to mixed-direction blocks were larger than the responses to adapted-direction blocks. Statistics on the response amplitudes were computed for each subject, for each visual area, across repeated scans and scanning sessions.

Acknowledgements

We thank W. Newsome for helpful comments. The research was supported by an NEI grant (RO1-EY12741) and a grant from the Human Frontier Science Program (RG0070/1999-B).

RECEIVED 27 JULY; ACCEPTED 29 OCTOBER 2001

1. Movshon, J. A., Adelson, E. H., Gizzi, M. S. & Newsome, W. T. The analysis of moving visual patterns. *Exp. Brain Res.* **11**, 117–152 (1986).
2. Rodman, H. R. & Albright, T. D. Single-unit analysis of pattern-motion selective properties in the middle temporal visual area (MT). *Exp. Brain Res.* **75**, 53–64 (1989).
3. Albright, T. D. Direction and orientation selectivity of neurons in visual area MT of the macaque. *J. Neurophysiol.* **52**, 1106–1130 (1984).
4. Li, B., Chen, Y., Li, B. W., Wang, L. H. & Diao, Y. C. Pattern and component motion selectivity in cortical area PMLS of the cat. *Eur. J. Neurosci.* **14**, 690–700 (2001).
5. Stoner, G. R. & Albright, T. D. Neural correlates of perceptual motion coherence. *Nature* **358**, 412–414 (1992).
6. Adelson, E. H. & Movshon, J. A. Phenomenal coherence of moving visual patterns. *Nature* **300**, 523–525 (1982).
7. Stoner, G. R., Albright, T. D. & Ramachandran, V. S. Transparency and coherence in human motion perception. *Nature* **344**, 153–155 (1990).
8. Welch, L. The perception of moving plaids reveals two motion-processing stages. *Nature* **337**, 734–736 (1989).
9. Welch, L. & Bowne, S. F. Coherence determines speed discrimination. *Perception* **19**, 425–435 (1990).
10. Kooi, F. L. *et al.* Properties of the recombination of one-dimensional motion signals into a pattern motion signal. *Percept. Psychophys.* **52**, 415–424 (1992).
11. Smith, A. T. Coherence of plaids comprising components of disparate spatial frequencies. *Vision Res.* **32**, 393–397 (1992).
12. Heeger, D. J., Boynton, G. M., Demb, J. B., Seidemann, E. & Newsome, W. T. Motion opponency in visual cortex. *J. Neurosci.* **19**, 7162–7174 (1999).
13. Gegenfurtner, K. R., Kiper, D. C. & Levitt, J. B. Functional properties of neurons in macaque area V3. *J. Neurophysiol.* **77**, 1906–1923 (1997).
14. Engel, S. A. & Furmanski, C. S. Selective adaptation to color contrast in human primary visual cortex. *J. Neurosci.* **21**, 3949–3954 (2001).
15. Grill-Spector, K. *et al.* Differential processing of objects under various viewing conditions in the human lateral occipital complex. *Neuron* **24**, 187–203 (1999).
16. Huk, A. C., Ress, D. & Heeger, D. J. Neuronal basis of the motion aftereffect reconsidered. *Neuron* **32**, 161–172 (2001).
17. Kourtzi, Z. & Kanwisher, N. Representation of perceived object shape by the human lateral occipital complex. *Science* **293**, 1506–1509 (2001).
18. Chawla, D. *et al.* Speed-dependent responses in V5: a replication study. *Neuroimage* **9**, 508–515 (1999).
19. Chawla, D., Phillips, J., Buechel, C., Edwards, R. & Friston, K. J. Speed-dependent motion-sensitive responses in V5: an fMRI study. *Neuroimage* **7**, 86–96 (1998).
20. Huk, A. C. & Heeger, D. J. Task-related modulation of visual cortex. *J. Neurophysiol.* **83**, 3525–3536 (2000).
21. Glover, G. H. & Lai, S. Self-navigated spiral fMRI: interleaved versus single-shot. *Magn. Reson. Med.* **39**, 361–368 (1998).
22. Nestares, O. & Heeger, D. J. Robust multiresolution alignment of MRI brain volumes. *Magn. Reson. Med.* **43**, 705–715 (2000).
23. Zeki, S. *et al.* A direct demonstration of functional specialization in human visual cortex. *J. Neurosci.* **11**, 641–649 (1991).
24. Tootell, R. B. *et al.* Functional analysis of human MT and related visual cortical areas using magnetic resonance imaging. *J. Neurosci.* **15**, 3215–3230 (1995).
25. Watson, J. D. *et al.* Area V5 of the human brain: evidence from a combined study using positron emission tomography and magnetic resonance imaging. *Cereb. Cortex* **3**, 79–94 (1993).
26. Engel, S. A., Glover, G. H. & Wandell, B. A. Retinotopic organization in human visual cortex and the spatial precision of functional MRI. *Cereb. Cortex* **7**, 181–192 (1997).
27. Engel, S. A. *et al.* fMRI of human visual cortex. *Nature* **369**, 525 (1994).
28. DeYoe, E. A. *et al.* Mapping striate and extrastriate visual areas in human cerebral cortex. *Proc. Natl. Acad. Sci. USA* **93**, 2382–2386 (1996).
29. Sereno, M. I. *et al.* Borders of multiple visual areas in humans revealed by functional magnetic resonance imaging. *Science* **268**, 889–893 (1995).
30. Smith, A. M. *et al.* Investigation of low frequency drift in fMRI signal. *Neuroimage* **9**, 526–533 (1999).